The Holocene

http://hol.sagepub.com/

Climatic control of the biomass-burning decline in the Americas after ad 1500

MJ Power, FE Mayle, PJ Bartlein, JR Marlon, RS Anderson, H Behling, KJ Brown, C Carcaillet, D Colombaroli, DG Gavin, DJ Hallett, SP Horn, LM Kennedy, CS Lane, CJ Long, PI Moreno, C Paitre, G Robinson, Z Taylor and MK Walsh

The Holocene 2013 23: 3 originally published online 14 August 2012
DOI: 10.1177/0959683612450196

Research paper

The Holocene
23(1) 3–13

DOI: 10.1177/0959683612450196
hol.sagepub.com
SAGE

Climatic control of the biomass-burning decline in the Americas after AD 1500

MJ Power,[1] FE Mayle,[2] PJ Bartlein,[3] JR Marlon,[4] RS Anderson,[5] H Behling,[6] KJ Brown,[7] C Carcaillet,[8] D Colombaroli,[9] DG Gavin,[3] DJ Hallett,[10] SP Horn,[11] LM Kennedy,[12] CS Lane,[13] CJ Long,[14] PI Moreno,[15] C Paitre,[16] G Robinson,[17] Z Taylor[11] and MK Walsh[18]

Abstract
The significance and cause of the decline in biomass burning across the Americas after AD 1500 is a topic of considerable debate. We synthesized charcoal records (a proxy for biomass burning) from the Americas and from the remainder of the globe over the past 2000 years, and compared these with paleoclimatic records and population reconstructions. A distinct post-AD 1500 decrease in biomass burning is evident, not only in the Americas, but also globally, and both are similar in duration and timing to 'Little Ice Age' climate change. There is temporal and spatial variability in the expression of the biomass-burning decline across the Americas but, at a regional–continental scale, 'Little Ice Age' climate change was likely more important than indigenous population collapse in driving this decline.

Keywords
biomass burning, charcoal, climate, human population, 'Little Ice Age'

Received 27 August 2011; revised manuscript accepted 22 March 2012

Introduction

Recent syntheses of sedimentary charcoal records suggest that biomass burning in the tropical Americas declined between AD 1500 and 1600 (Bush et al., 2008; Dull et al., 2010; Nevle and Bird, 2008). However, the geographic extent, magnitude, and cause of this decline are uncertain because of the limited geographic coverage and temporal resolution of available data, as well as incomplete evaluation of all potential controls in these syntheses. Proponents of the population-collapse hypothesis (PCH) (Dull et al., 2010; Nevle and Bird, 2008) argue that this decline reflects a reduction in anthropogenic biomass burning due to decimation of indigenous populations by diseases, such as smallpox, following European contact. If the PCH is correct, this implies that the pre-Columbian (pre-AD 1492) fire regime of tropical ecosystems was largely anthropogenic, consistent with the 'cultural parkland' hypothesis (Erickson, 2000; Heckenberger et al., 2003), and that post-Contact (post-AD1492) indigenous population collapse resulted in 'reforestation' owing to a reduction in anthropogenic ignitions. This scenario has been used to explain declines in atmospheric $\delta^{13}CH_4$ (Ferretti et al., 2005; Mischler et al., 2009), CO (Wang et al., 2010) and CO_2 concentrations (Frank et al., 2010; Ruddiman et al., 2011) between AD 1600 and 1700 (Dull et al., 2010; Faust et al., 2006). An alternative, but not mutually exclusive, explanation (the climate change hypothesis, CCH) proposes that climatic variations were largely responsible for this decline in tropical biomass burning (Marlon et al., 2008; Pechony and Shindell, 2010).

Here, we examine the PCH and CCH for the post-AD 1500 decline in biomass burning in the Americas by synthesizing charcoal series spanning the last 2000 years (2 kyr) from an updated version of the Global Charcoal Database (GCD) (Power et al., 2008) (Figure 1), and comparing these with reconstructions of climate and population (Goldwijk et al., 2010; Mann et al., 2009). To examine the implicit prediction of the PCH that the post-AD 1500 decline in biomass burning in the Americas was globally unique, we compared the composite 2-kyr charcoal curve for the Americas with that of the rest of the world ('non Americas').

[1]University of Utah, USA
[2]University of Edinburgh, UK
[3]University of Oregon, USA
[4]University of Wisconsin, USA
[5]Northern Arizona University, USA
[6]Georg-August University, Germany
[7]Canadian Forest Service, Canada
[8]École Pratique des Hautes Études, France
[9]University of Bern, Switzerland
[10]Biogeoscience Institute, University of Calgary, Canada
[11]University of Tennessee, USA
[12]Virginia Tech, USA
[13]University of North Carolina Wilmington, USA
[14]University of Wisconsin Oshkosh, USA
[15]Universidad de Chile, Chile
[16]Université Laval, Canada
[17]Fordham College at Lincoln Center, USA
[18]Central Washington University, USA

Corresponding author:
MJ Power, NHMU, Department of Geography, University of Utah, Salt Lake City, Utah, USA.
Email: mitchell.power@geog.utah.edu

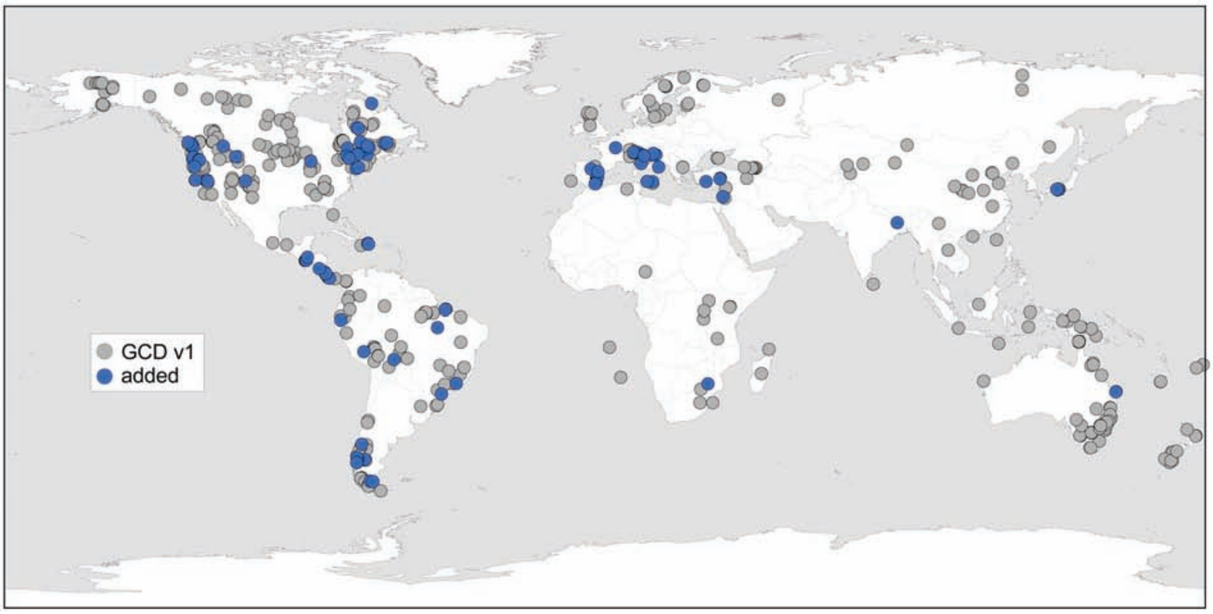

Figure 1. Global map showing locations of charcoal records from version 1 (gray circles) of the Global Charcoal Database (GCD) (Power et al., 2010) and new records (blue circles) incorporated into this study. Charcoal records from the Americas not included in GCD v1 were obtained: (1) as raw data from data contributors (included here as co-authors), (2) by digitizing previously published charcoal records, and (3) from data contributed to previously published charcoal syntheses (Table 1).

Materials and methods

Charcoal data sources

We obtained 498 sedimentary charcoal records covering part or all of the last two millennia from the Global Charcoal Database (GCD version 1), co-author contributions, and from published syntheses (Marlon et al., 2008; Vannière et al., 2011). The GCD contains charcoal records from lacustrine, fen, bog, marine, archaeological, and other sites. We intentionally excluded non-terrestrial charcoal records, including marine sediments, and records from alluvial fans and soils (Carcaillet, 2001), because of the challenges of temporally constraining these types of deposits. In an attempt to improve our geographic coverage of late-Holocene fire activity across the Americas, an additional 84 charcoal records (Table 1, Figure 1) were acquired from contributors to the GCD or by digitizing records from the published literature. Uncalibrated radiocarbon dates from new (additional) records were calibrated according to the protocol established for inputting data (Power et al., 2008) for consistent treatment to all radiocarbon-dated chronologies.

Statistical/numerical analyses of charcoal data

To make charcoal data comparable from a wide range of sampling, processing, and quantification techniques from hundreds of sites, we used a protocol that normalizes individual records in order to stabilize the variance and standardize the results (Power et al., 2008, 2010). Composite records were created by smoothing the standardized records using a two-stage smoothing process (Power et al., 2010). First, individual records were sampled and smoothed by selecting all data points within each 20-year interval in a record and calculating a locally weighted mean ('lowess') based on a tricube weight function, which weights the middle 10 years of the window most heavily (Cleveland and Devlin, 1988). If no data points existed within a given 20-year window, no interpolation was performed, which is important because it avoids creating data through interpolation rather than observation. In the second smoothing step, samples from all records with data for a given 100-year interval were combined and used to calculate the lowess regression. In this latter step, a 'robustness iteration' was performed that minimizes the influence of extreme charcoal values, providing an estimate of the sample mean that is robust to outliers. This methodology emphasizes long-term trends in the charcoal data that are characteristic of multiple records. Confidence intervals for each composite curve were generated by a bootstrap re-sampling (with replacement) of individual sites (not samples) over 1000 replications. Bootstrap confidence intervals for each target point were taken as the 2.5th and 97.5th percentiles of the 1000 fitted values for that target point.

Trends in population estimates were constructed by summarizing the HYDE 3.1 data set (Goldwijk et al., 2010) by geographic region (as shown in Figure 2) Population time series were generated by areally averaging gridded HYDE data over the same region used for compositing and summarizing charcoal series. Regional reconstructions for temperature and precipitation data were obtained from a variety of published sources (see Figure 4). These climate time series were smoothed using the same approach taken with the charcoal data (i.e. lowess smoothing based on a 150-year window width).

Archaeological site locations

Locations of large (~ >1 km^2) archaeological sites were obtained from the United Nations Educational, Scientific and Cultural Organization (UNESCO) and from available literature, regional and local park services, and data available through the World Wide Web. UNESCO sites are considered 'of outstanding universal value' by the World Heritage Committee and are available through their web page (http://whc.unesco.org/en/criteria). All sites were separated into two temporal categories: (1) prehistoric sites (i.e. sites that were occupied between AD 1250 and 1500), and (2) sites occupied prior to AD 1250. Site names and locations

Table 1. Charcoal records compiled for this analysis and added to the version 1 of the Global Charcoal Database.

Charcoal record	GCD Site #	Site name	Latitude	Longitude	Elevation	Data source
1	54	Martins	47.713	−123.54	1415	RAW – D Gavin
2	55	Moose	47.883	−123.35	1508	RAW – D Gavin
3	76	Laguna Venus	–45.533	−72.01	600	DIGI – Sceicz et al. (1998)
4	133	Deherrara	37.741	−107.708	3343	RAW – RS Anderson
5	157	Potrok Aike	–51.966	−70.383	100	DIGI – Haberzettl et al. (2006)
6	201	Porphyry	48.905	−123.833	1100	RAW – K Brown
7	202	Walker	48.529	−124.002	950	RAW – K Brown
8	204	Lagoa da Curuca	-0.766	−47.85	35	RAW – H Behling
9	205	Albion	45.671	−71.325	320	RAW – C Carcaillet
10	206	Castor	46.613	−72.998	220	RAW – C Carcaillet
11	207	Desautels	49.457	−73.25	480	RAW – C Carcaillet
12	208	Dolbeau	48.966	−65.955	965	RAW – C Carcaillet
13	209	J'Arrive	49.247	−65.376	56	RAW – C Carcaillet
14	210	Madeleine	47.666	−70.719	800	RAW – C Carcaillet
15	211	Neume	47.587	−77.11	363	RAW – C Carcaillet
16	312	Lac Hertel	45.683	−74.05	75	RAW – K Brown
17	362	Turtle	49.32	−124.95	80	RAW – K Brown
18	366	Lac Diana	60.988	−69.958	114	RAW – K Brown
19	554	Canal de la Puntilla	−40.95	−72.9	120	RAW – P Moreno
20	596	El Carrizal	41.31911	−4.14373	860	Vannière et al. (2011)
21	597	Allom	−25.23	153.17	100	Marlon et al. (2008)
22	600	Funduzi	−22.86	30.89	429	Marlon et al. (2008)
23	610	Teletskoye	25.23	87.65	1900	Marlon et al. (2008)
24	611	Griblje Marsh	45.56972	15.27917	160	Vannière et al. (2011)
25	612	Canada de la Cruz	38.4	−2.42	1595	Vannière et al. (2011)
26	613	Villaverde	38.8	−2.22	870	Vannière et al. (2011)
27	614	Baza	37.2333	−2.7	1900	Vannière et al. (2011)
28	615	Mlaka	45.50278	15.20556	150	Vannière et al. (2011)
29	616	El Tiro Bog	−3.84	−79.145	2810	DIGI – Niemann and Behling (2008)
30	621	Bao-1	19.066	−71.033	1775	RAW – L Kennedy and S Horn
31	622	Laguna Azul	−52.12	−69.522	100	DIGI – Mayr et al. (2005)
32	623	Crevice Lake	45	−110.578	1713	RAW – M Power
33	624	Comailles	47.66	3.22	215	Marlon et al. (2008)
34	627	Gádor	36.9	−2.91667	1530	Vannière et al. (2011)
35	634	Lago di Gembro	46.16444	10.15444	1350	Vannière et al. (2011)
36	639	Ojos del Tremendal	40.53333	−2.05	1650	Vannière et al. (2011)
37	672	Mizorogaike	35.06	135.77	75	Marlon et al. (2008)
38	673	Jagaike	35.24	135.46	640	Marlon et al. (2008)
39	713	Bereket Basin	37.54518	30.29506	1410	Vannière et al. (2011)
40	714	Lago di Pergusa	37.51667	14.3	674	Vannière et al. (2011)
41	769	Little Lake	44.168	−123.583	703	RAW – C Long
42	772	Eski Acigöl	38.55	34.54	1270	Vannière et al. (2011)
43	773	Nar	38.37	34.45	1363	Vannière et al. (2011)
44	824	Lago Lucone	45.55	10.4833	249	Vannière et al. (2011)
45	825	Pian Segna	46.1805	8.6397	1162	Vannière et al. (2011)
46	826	Lago di Fimon	45.4666	11.5333	23	Vannière et al. (2011)
47	827	Piano	46.3208	8.62	1439	Vannière et al. (2011)
48	833	Prapoce	45.4236	14.075	480	Vannière et al. (2011)
49	848	Gorgo Basso	37.6166	12.65	6	Vannière et al. (2011)
50	851	Amont	53.733	−74.383	335	RAW – P Cedric
51	852	Aval	53.416	−73.866	335	RAW – P Cedric
52	854	Lac des Ilets	48.197	−71.242	120	DIGI – Simard et al. (2006)
53	864	Resnikov prekop	45.975	14.54306	290	Vannière et al. (2011)
54	889	Beaver 2	44.917	−123.305	69	RAW – M Walsh
55	1061	Laguna Verde	13.891	−89.786	1600	RAW – R Dull
56	1062	Laguna Cuzcachapa	13.986	−89.681	709	RAW – R Dull
57	1063	Laguna Llana del Espino	13.95	−89.52	700	RAW – R Dull
58	1064	Laguna Santa Elena	8.56	−82.56	1100	DIGI – Anchukaitis and Horn (2005)
59	1065	Marcacocha	−13.218	−72.208	3355	DIGI – Chepstow-Lusty et al. (1998)
60	1069	Laguna Lincoln	−45.366	−74.066	19	RAW – S Lumley
61	1070	Laguna Lofel	−44.928	−74.325	13	RAW – S Lumley
62	1071	Laguna Six Minutes	−46.416	−74.333	15	RAW – S Lumley

(Continued)

Table 1. (Continued)

Charcoal record	GCD Site #	Site name	Latitude	Longitude	Elevation	Data source
63	1072	Laguna Stibnite	−46.416	−74.4	15	RAW – S Lumley
64	1076	Carajas	−6	−50.1605	250	DIGI – Cordiero et al. (2008)
65	1077	Lower Gaylor Lake	37.908	−119.286	3062	RAW – D Hallett
66	1078	Barrett Lake	37.595	−119.006	2816	RAW – D Hallett
67	1079	Lago de Accesa	42.988	10.894	155	Vannière et al. (2011)
68	1090	Crevice Lake	45	−110.578	1713	RAW – M Power
69	1092	Graham lake	45.183	−77.35	381	DIGI – Fuller (1997)
70	1093	High lake	44.516	−76.6	192	DIGI – Fuller (1997)
71	1095	Aracatuba	−25.916	−48.983	1500	RAW – H Behling
72	1098	Serra da Bocaina 1	−22.741	−44.556	1500	RAW – H Behling
73	1099	Binnewater	41.41	−74.551	256	RAW – G Robinson
74	1100	Hyde Park	41.78	−73.893	74	RAW – G Robinson
75	1113	Battaglia	41.905	16.134	0	Vannière et al. (2011)
76	1114	Hula	33.04	35.37	70	Vannière et al. (2011)
77	1116	Lago della Costa	45.27	11.742	7	Vannière et al. (2011)
78	1120	Foy Freeze Core	48.165	−114.359	1006	RAW – M Power
79	1121	Aguada de Petapilla	14.867	−89.125	710	DIGI – Rue et al. (2002)
80	1122	Cantarrana	10.439	−84.006	36	RAW – Kennedy and Horn
81	1128	Three Creeks	44.099	−121.627	1996	RAW – C Long
82	1129	Todd Lake	44.027	−121.684	1875	RAW – C Long
83	1130	Tumalo Lake	44.021	−121.543	1536	RAW – C Long
84	1131	Bulter Lake	43.662	−88.134	316	RAW – C Long
85	1132	Seven Lake	43.613	−88.134	396	RAW – C Long
86	1133	Laguna Bonillita	9.993	−83.6131	450	RAW – S Horn
87	1143	Charco Verde	11.476	−85.631	37	RAW – R Dull
88	1148	Upper Squaw Lake	42.033	−123.015	930	RAW – D Colombaroli
89	1155	Wildcat Lake	37.968	−122.785	67	RAW – RS Anderson
90	1156	Glenmire	37.993	−122.776	400	RAW – RS Anderson
91	1157	Yaguarú	−15.6	−63.216	399	RAW – Z Taylor and S Horn
92	1158	Salvador	18.795	−70.886	990	RAW – S Horn and C Lane
93	1159	Castilla	18.795	−70.875	976	RAW – C Lane and S Horn

shown in Figure 2 were not intended to be comprehensive, but depict the broad geographic distribution of important and well documented archaeological site locations.

Results and discussion

Linkages among biomass burning in the Americas, the rest of the world, and global biogeochemical cycling and climate change

The composite curve for the Americas (Figure 3a) shows a decrease in charcoal influx (biomass burning) between AD 1500 and 1650, with a minimum between AD 1650 and 1700, the lowest level for the past 6 kyr (see Figure 5). There is also a prominent local minimum in the non-Americas composite curve (Figure 3b) of similar duration to that in the Americas, but its onset and maximum expression occurs about 100 years earlier. Although the timing of this minimum in the Americas is consistent with the general chronology of population (Figure 3e,f) associated with the arrival and spread of European diseases across the hemisphere (Denevan, 1992), the slightly earlier parallel decline outside the Americas is impossible to explain through population collapse in the Americas. A climate-driven reduction in biomass burning can, however, explain both declines, as well as the difference in timing between them inasmuch as changes in atmospheric circulation associated with the 'Little Ice Age' (LIA), defined by maximum global cooling AD 1400–1700 (Mann et al., 2009), were not globally uniform or synchronous.

The low levels of biomass burning between ~ AD 1500 and 1750 have been used to explain some striking features in ice-core records of global biogeochemical cycles. In particular, atmospheric CO_2 concentrations (Figure 3i) decreased by around 5 ppm between AD 1500 and 1700 (Frank et al., 2010; Joos and Spahni, 2008), a pattern attributed by others (Dull et al., 2010; Faust et al., 2006; Ruddiman et al., 2011) to increased carbon sequestration in the Americas related to population collapse. Similarly, the record of $\delta^{13}CH_4$ (Figure 3g), which includes biomass burning as one of the source terms in its budget, also shows a steep decline between AD 1400 and 1750, and this too has been ascribed to a decrease in biomass burning in the Americas following population collapse (Ferretti et al., 2005; Mischler et al., 2009). The ice-core record of CO from combustion sources also shows a broad decrease from AD 1350 to 1650, followed by an increase (Wang et al., 2010), attributed to variations in Southern Hemisphere biomass burning. It is clear, however, that a *global* reduction in biomass burning (Figure 3a,b) prevailed between AD 1500 and 1750, and, crucially, the declines in CO_2 and $\delta^{13}CH_4$ were already underway by AD 1200 and AD 1400, respectively. The proposal that carbon sequestration in the Americas (and elsewhere) may have contributed to the sharpness of the decreases in CO_2 between AD 1500 and 1700 (e.g. from 280 to 275 ppm) is not supported by simulations with coupled climate-carbon cycle models (Pongratz et al., 2011), even if exaggerated estimates of the potential land-cover change are used. Similarly, land-cover changes, either 'best estimates' or larger, cannot explain the

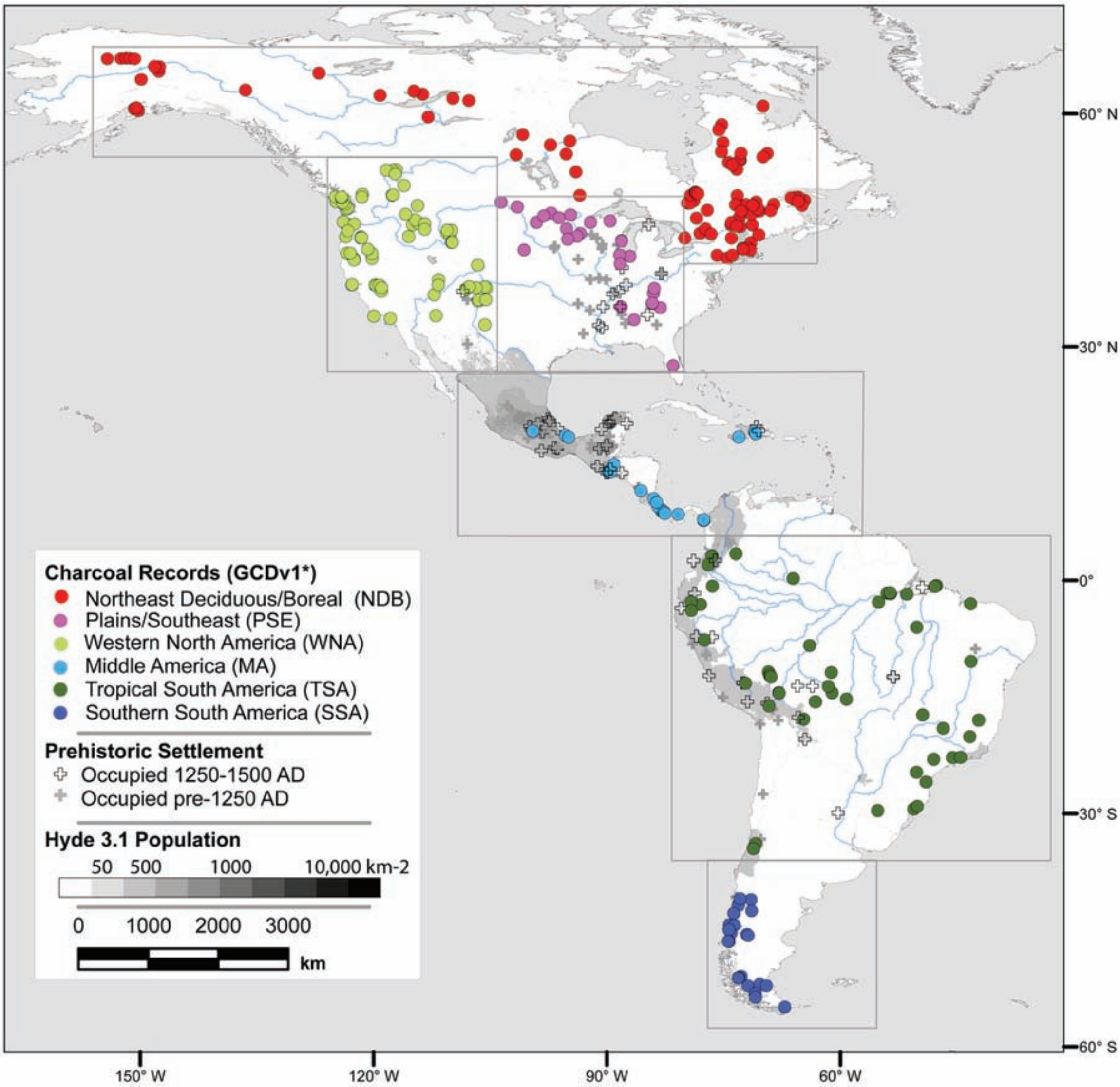

Figure 2. Map of the Americas showing locations of 302 charcoal records used for generating the composite 2-kyr charcoal curves for the entire Americas (Figure 3a) and its constituent (color-coded) regions (Figure 4a–e and Figure 6). Key Pre-Columbian archaeological sites are shown (see methods). Population estimates (Goldwijk et al., 2010) are shown for AD 1400.

longer-term (Holocene) trends (Stocker et al., 2011), and similar arguments could be made for the trends in $\delta^{13}CH_4$ and CO. Moreover, the global expression of the biomass-burning reduction in the charcoal evidence implies that there is no particular reason to ascribe the trends in greenhouse gas concentrations in the ice-core records to biomass-burning changes either in the Americas or in the Southern Hemisphere alone, as opposed to ascribing them to global changes.

The potential controls of the global decrease in biomass burning between AD 1500 and 1750 can be inferred both by direct comparison with climatic reconstructions (Mann et al., 2009) and through biomass-burning simulation studies (Pechony and Shindell, 2010). Annual mean temperatures were generally decreasing over the 1000 years prior to the interval of low biomass burning, both in the Americas and elsewhere (Figure 3), with temperatures in the Americas reaching a local minimum after those elsewhere (i.e. AD 1650 versus 1500), parallel in timing with the minima in the charcoal curves. Temperature, through its influence on vegetation productivity, and hence fuel, is the primary control of biomass burning on long timescales and large spatial scales (Harrison et al., 2010). The 'non-Americas' biomass-burning curve increases from AD 1000 to 1400, in opposition to the temperature curve, and is driven largely by an increase in biomass burning in the southern extra-tropics, in particular Australia (Marlon et al., 2008; Mooney et al., 2011). A recent simulation study (Pechony and Shindell, 2010) explains this upturn via increasing precipitation in the southern extra-tropics over this interval. In temperate Australia, where biomass burning is limited by moisture-controlled fuel availability (Mooney et al., 2011), an increase in effective moisture increases burning. Other aspects of these simulations (Pechony and Shindell, 2010) bear on the issues here – the interval of globally lower biomass burning observed in the charcoal data is well expressed both globally and regionally in simulations that either include or exclude a parameterization of the effects of population density on ignition and suppression of fire. The similarity in the trends in biomass burning in the Americas and elsewhere, the particular timing of the local minima, and the straightforward explanation for these in climate terms, suggest

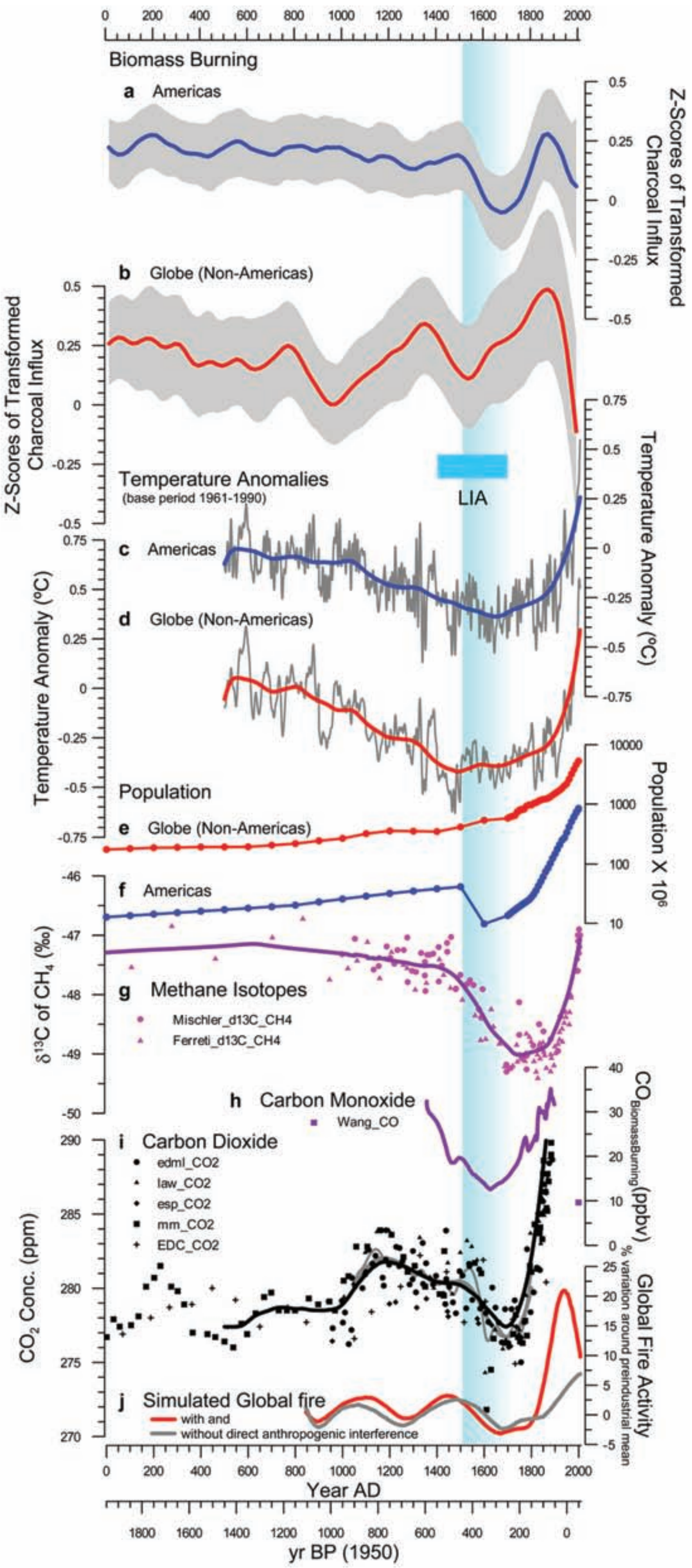

Figure 3. 2-kyr composite series of biomass burning, expressed as 150-yr, lowess-smoothed, Z scores of transformed charcoal influx, for the Americas (a) and the 'non-Americas' (GCD vs. 1 (Power et al., 2008)) (b), plotted against temperature anomalies (Mann et al., 2009) for the Americas (c) and 'non-Americas' (d), and for the Hyde 3.1 human population estimates (Goldwijk et al., 2010) for the Americas (f) and 'non-Americas' (e). The period of the 'Little Ice Age', shown as a blue bar, is defined as AD 1400–1700 (Mann et al., 2009). Values for methane isotopes, δ^{13}C of CH_4 (Ferretti et al., 2005; Mischler et al., 2009), are expressed as a 150-yr lowess smoothed (g). The magenta bar, labeled T3, is the interval of AD 1589–1730, argued by Ferretti et al. (2005) and Mischler et al. (2009) to be a period when population collapse led to decreasing biomass burning. Also shown are ice-core derived carbon monoxide (h) (Wang *et* al., 2010) and CO_2 values (i) for 'edml_CO2' (Siegenthaler et al., 2005), 'Law_CO2' (Etheridge et al., 2001), 'esp_CO2' (Siegenthaler et al., 2005), 'mm_CO2' (MacFarling et al., 2006), and 'EDC_CO2' (Monnin et al., 2004). The black line in (i) is a 150-yr lowess-smoothing of all CO_2 records (allowing comparison with the smoothed charcoal time series); the gray lines show 50- and 150-yr smoothing-spline curves as used in Frank et al. (2010), which do not down-weight outliers as in the Lowess smoothing. Similar to Frank et al. (2010), CO_2 values are plotted only up to 290 ppm. Modeled global fire (j) shows simulations with (red line) and without (gray line) direct anthropogenic influence (ignition and suppression) (Pechony and Shindell, 2010). The vertical blue gradient, beginning at AD 1500, provides a visual guide. See Figure 2 and Table 1 for locations of charcoal records, and Power et al. (2008, 2010) for discussion of methods.

that the interval of lower biomass burning in the Americas between ~ AD 1500 and 1750 is parsimoniously explained by the CCH.

Regional patterns of biomass burning, climate change, and population in the Americas

Analysis of regional 2-kyr charcoal series (Figures 4 and 6) across the Americas allows further consideration of the relative merits of the two hypotheses. If the PCH is correct, one would predict that the highest amplitude, and earliest, post-contact charcoal decline would have occurred in tropical Middle America (MA), where indigenous populations were highest (Denevan, 1992; Goldwijk et al., 2010) (Figures 2 and 4) and where their collapse through introduction of European diseases (Denevan, 1992) first began. Conversely, middle-to-high latitude regions would be expected to have experienced relatively more subtle, and later, post-contact declines in biomass burning because of their relatively lower population densities (Figures 2 and 4) and later arrival of European diseases. However, our results do not show this. Instead we find that sparsely populated (Denevan, 1992; Goldwijk et al., 2010) southern South America (SSA) experienced a major decline in biomass burning, commencing sharply at AD 1550, and of comparable magnitude to that of MA. Furthermore, the charcoal decline in MA began at ~ AD 1350, preceding European contact by 150 years (Figures 4d and 6). Similarly, in western North America (WNA), the onset of the charcoal decline also preceded European contact, beginning at ~AD 1450 (Figures 4c and 6, see also Marlon et al., 2012). The charcoal curve for tropical South America (TSA) also does not conform to the predictions of the PCH. Instead of a major downturn, there was only a subtle decline in biomass burning in TSA, which did not begin until AD 1700, *c.* 200 years after European contact (Figures 4e and 6).

Despite this inter-regional variability in the initial onset, and magnitude, of charcoal declines, our data show a consistent post-AD 1500 charcoal minimum across the Americas, centered between AD 1600 and 1750, that correlates with the height of the LIA (Figures 3 and 6), suggesting a regional- to hemispheric-scale climatic explanation for this charcoal minimum. The climatic expression of the LIA across the Americas (Figure 4), however, is heterogeneous, not only in terms of cooling intensity (relatively greater in the mid-high latitudes; Mann et al., 2009; Mooney et al., 2011), but also precipitation, which, for example, decreases in MA (Figure 4d) but increases in Patagonia (Mayr et al., 2005; Meyer and Wagner, 2009; Moy et al., 2008).

The spatial-temporal variability in LIA climate change, together with large-scale differences in vegetation type, fuel load and flammability, and indigenous population density (Figure 2), undoubtedly caused regional variations in biomass burning across the Americas. The low pre-Columbian population densities in high latitudes, including the northeast deciduous/boreal forest (NDB) and Patagonia (SSA) (Denevan, 1992; Goldwijk et al., 2010), is inconsistent with the PCH as an explanation for the high-amplitude steep charcoal declines there (Figures 4a,f and 6). Correlation between temperature and charcoal minima for NDB between AD 1600 and 1800 (Figure 4a) suggests that cooler temperatures reduced fuel flammability, and possibly also lowered the prevalence of lightning (an important ignition source in boreal forests today (Food and Agriculture Organization (FAO), 2007), and thereby decreased biomass burning then. In SSA the charcoal

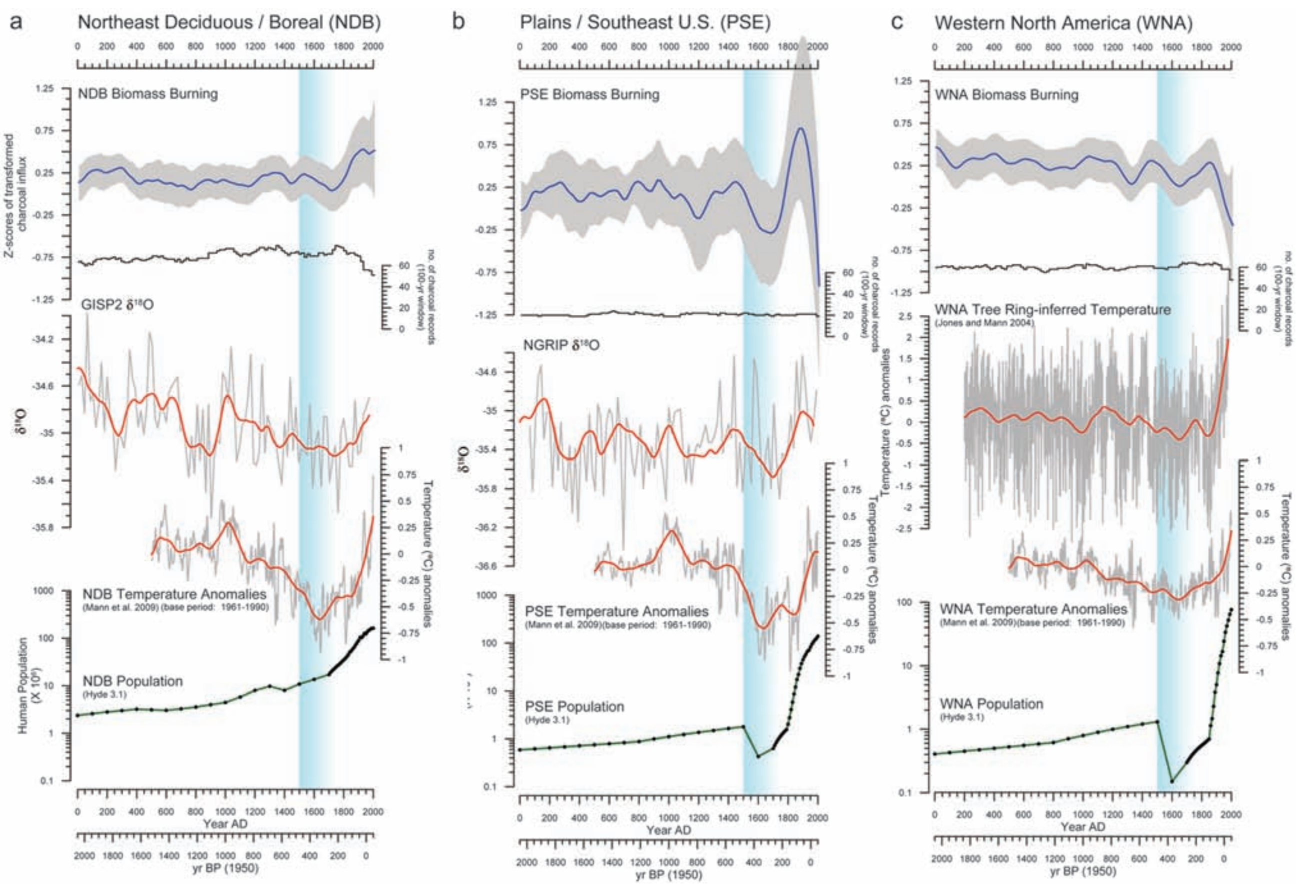

(Continued)

Figure 4. Continued

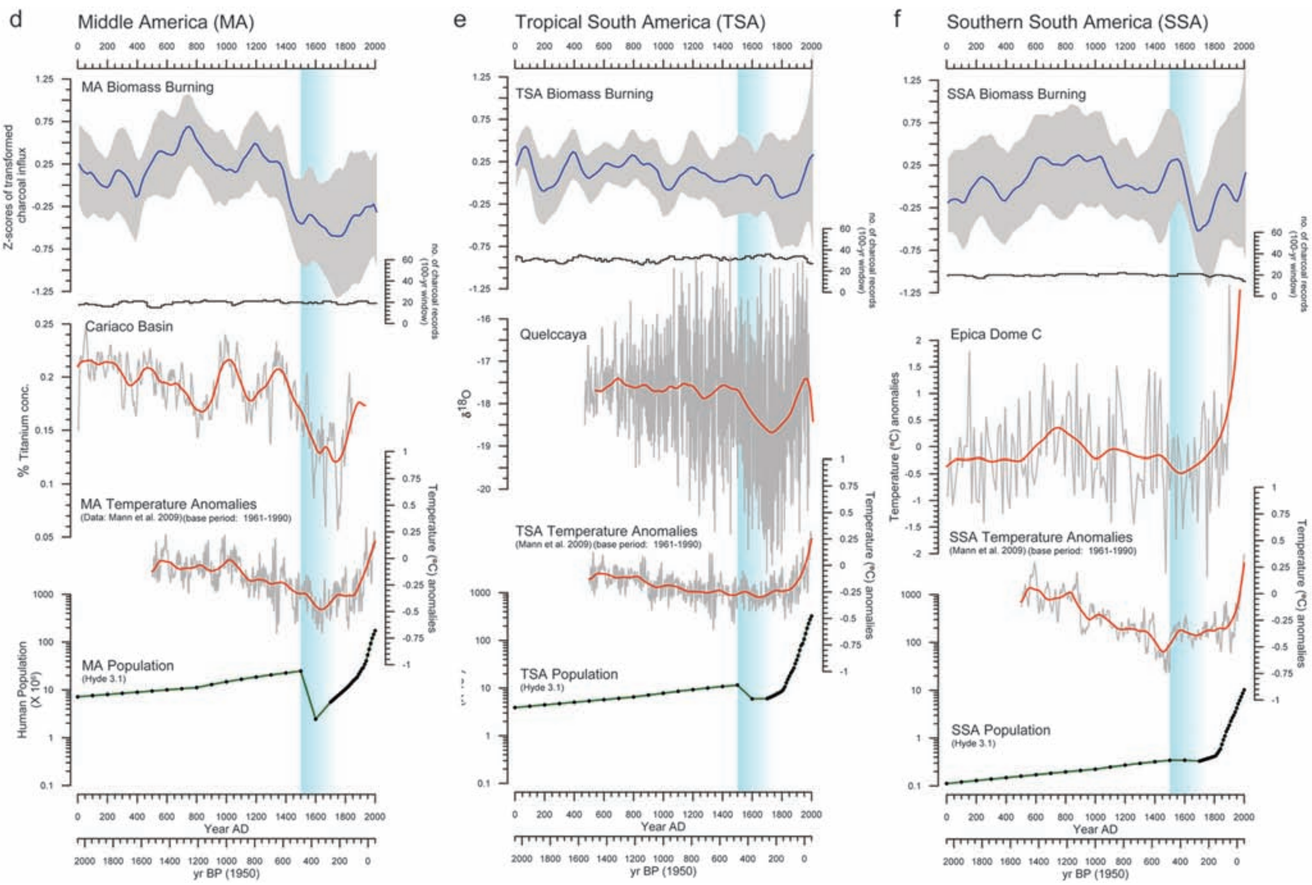

Figure 4. 2-kyr composite time-series of 100-year smoothed Z-score charcoal anomalies from six constituent regions (Figure 2) of the Americas. Geographic headings for the selected regions of the Americas include: (a) Northeast deciduous and Boreal region, (b) Plains and southeastern USA, (c) Western North America, (d) Middle America, (e) tropical South America, and (f) southern South America, and are presented with climate and population data. The upper and lower 95% confidence intervals are shown in gray and the number of charcoal samples contributing to each overlapping 100-year window in the bootstrap analysis is shown below each regional composite charcoal time series. Each regional biomass-burning composite is plotted against 100-year smoothed, regionally averaged, climate and human population data. Regionally summarized Hyde 3.1 (Goldwijk et al., 2010) population data, providing an aerially averaged estimate of population per region, are shown at the bottom of each regional panel. Climate reconstructions are aerially averaged paleotemperature reconstructions used in Mann et al. (2009). Proximal paleoclimate proxies of temperature and moisture variability from previously published studies are also shown for each region: Greenland Ice Sheet Project 2 (GISP2: Stuiver et al., 1997), Greenland summit ice-core $\delta^{18}O$ (NGRIP, 2006), western North America tree-ring based temperatures (Jones and Mann, 2004), Cariaco basin titanium concentrations (as a proxy for precipitation) (Haug et al., 2001), and Quelccaya ice-core $\delta^{18}O$ (Thompson et al., 1985).

minimum between AD 1600 and 1800 correlates more closely with peak precipitation than lowered temperature (Figure 4f; Mayr et al., 2005; Meyer and Wagner, 2009; Moy et al., 2008), which also would have reduced fuel flammability, and thereby suppressed biomass burning. The similarity among decreasing Greenland LIA temperatures and western US tree-ring-inferred temperatures and decreasing biomass burning across temperate North America (WNA and the Plains/SE USA (PSE)) (Figure 4b,c) also supports the LIA CCH.

The differing patterns of charcoal decline between tropical MA versus TSA are intriguing. In MA the charcoal decline began well before European contact and correlates well with the LIA declines in both temperature (Mann et al., 2009) and precipitation (Figure 4d), providing stronger support for the CCH than the PCH. The precipitation decline in MA (Cariaco record, Haug et al., 2001) correlates with a decrease in biomass burning, suggesting that a prolonged reduction in rainfall would have limited fuel availability in drier tropical ecosystems (Archibald et al., 2009). The Caribbean Cariaco record may not adequately capture the spatial complexity of climate across MA or LIA cooling, considering that fire is most common in tropical systems with intermediate levels of fuel loads and precipitation. A more detailed study of MA records, at higher spatio-temporal resolution, encompassing differences in vegetation, topography, and climate, is needed to explore the relationship between LIA climate change and biomass burning in this region of the Americas.

The relative importance of the LIA versus the PCH in explaining the charcoal decline in TSA is less clear than in MA because there is only a minor post-AD 1500 charcoal decline in TSA, beginning *c*. AD 1700 (Figures 4e and 6), which significantly postdates both the onset of the LIA in the region as well as the post-contact population collapse (Denevan, 1992) (Figure 4e). Therefore, neither climate change nor demographic collapse had a strong influence on post-AD 1500 biomass burning in TSA. The absence of a clear driver for the TSA biomass-burning signal may reflect the large seasonal and interannual variations in climate, vegetation and topography across this vast region – encompassing humid rainforest, cloud forest, seasonally dry forest, savannas, and paramo, and climatic regimes from ever-wet to arid and lowland tropical to alpine. Today, climatic phenomena such as the El

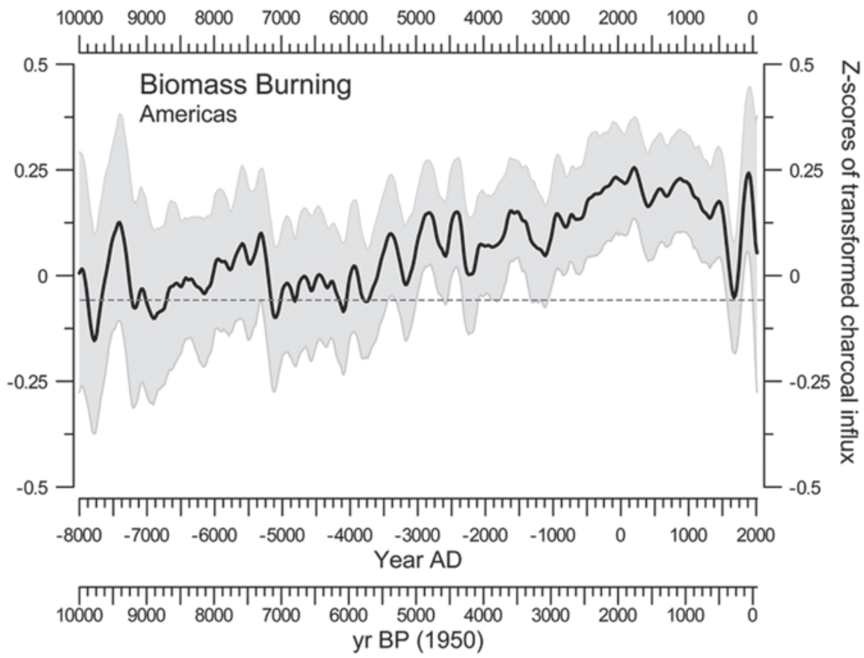

Figure 5. 10-kyr composite time-series of 150-year smoothed Z-score charcoal anomalies (CHAR) from all charcoal records in the Americas. The upper and lower 95% confidence intervals are shown in gray and the dashed horizontal line marks the 17th century LIA biomass-burning minima, the largest negative Z-score charcoal anomaly during the past six millennia.

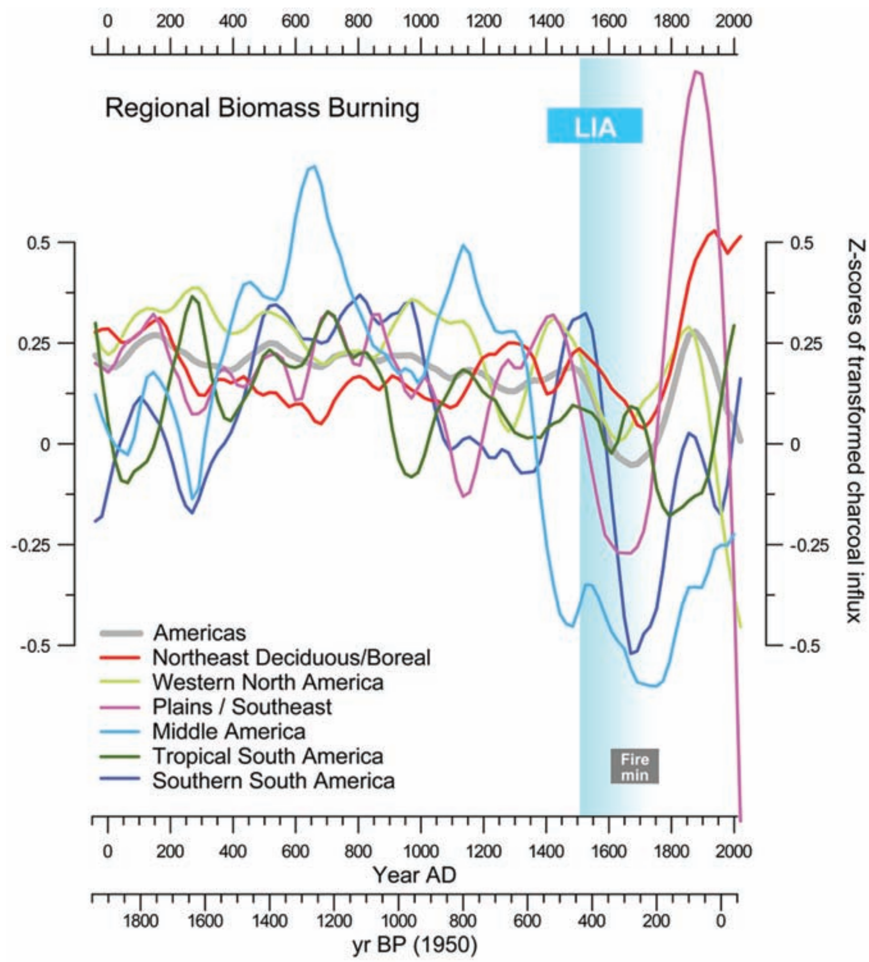

Figure 6. 2-kyr composite series of 100-year smoothed Z-score charcoal anomalies (CHAR) from five constituent regions (Figure 2) of the Americas. The LIA, as defined by (Mann et al., 2009), is shown by the vertical blue bar; the biomass-burning minima for the entire Americas, centered ~ AD 1600–1750, is shown as a gray box.

Niño Southern Oscillation (ENSO) have markedly spatially heterogeneous impacts in terms of precipitation across TSA (drought in some areas, increased rainfall in others) (Garreaud et al., 2009; Nepstad et al., 2004), in which case the LIA may well have also had different climatic impacts across the region. Furthermore, even under the same directional shift in precipitation, different vegetation types across TSA may have had opposite responses in terms of the amount of biomass burnt – e.g. an increase in dry season precipitation causing an increase in biomass burnt in moisture-limited savanna and caatinga (cactus thorn-scrub) as fuel load increases, but decreases in biomass burnt in seasonally dry forest as flammability decreases (Archibald et al., 2009; Nepstad et al., 2004).

Even at the local scale, Bush et al. (2007) found that neighboring sites, within a few kilometers of each other, can yield markedly different charcoal time-series. However, given that these lakes in the Peruvian Amazon have the same climatic regime, soils, and vegetation type (humid rainforest), variability in biomass burning was interpreted, not as climate-driven, but reflecting highly localized patterns of pre-Columbian anthropogenic rainforest burning (Bush et al., 2007).

Conclusions

We conclude that, although there are regional differences in the timing and pattern of biomass burning trends, there is a broadly consistent post-AD 1500 decrease in biomass burning across the Americas, which is most consistent with LIA climate change as the predominant driver or first order control at a regional to hemispheric scale. This implies that pre-Columbian indigenous peoples did not exert as strong an influence upon large-scale biomass burning as previously supposed. However, our findings do not preclude the possibility that post-contact population collapse may have been a more important control at smaller/finer spatial scales (e.g. evident from tight clusters of lakes in Peruvian Amazonia, Bush et al., 2007), or that the magnitude of the post-AD 1500 charcoal decline, especially in the densely populated tropics (MA) (Denevan, 1992), may have been amplified by the impact of post-contact population collapse. Our findings also show that the 16th-century downturn in biomass burning was not unique to the Americas, but was a global phenomenon that was underway well before AD 1500. Consequently, the minima in ice-core trace-gas indicators of biomass burning, and in atmospheric carbon dioxide concentrations, after AD 1500 should not be attributed to post-contact decreases in anthropogenic biomass burning and consequent increases in carbon sequestration in the Americas.

Acknowledgements

We thank data contributors to the GCD, including contributions from Robert Dull and Susie Lumley, the Global Palaeofire Working Group (GPWG) of the International Geosphere-Biosphere (IGBP) Cross-Project Initiative on Fire, and the UK Natural Environment Research Council QUEST-Deglaciation and QUEST-Desire projects for funding. Author contributions**:** MJP, FEM, PJB and JRM developed the ideas; MJP, FEM, PJB designed the analyses, and wrote the initial drafts of the paper. MJP and PJB carried out the analyses; MJP and JRM collected data, created age models and entered data into the Global Charcoal Database (GCD). The remaining authors contributed new data to the GCD. All co-authors contributed equally to the final drafting of the paper.

Funding

This study was supported by the UMNH (MJP) and the US National Science Foundation (PJB).

References

Anchukaitis KJ and Horn SP (2005) A 2000-year reconstruction of forest disturbance from southern Pacific Costa Rica. *Palaeogeography, Palaeoclimatology, Palaeoecology* 221: 35–54.

Archibald S, Roy DP, van Wilgen BW et al. (2009) What limits fire? An examination of drivers of burnt area in southern Africa. *Global Change Biology* 15: 613–630.

Bush MB, Silman MR, de Toledo MB et al. (2007) Holocene fire and occupation in Amazonia: Records from two lake districts. *Philisophical Transactions of the Royal Society B* 362: 209–218.

Bush MB, Silman MR, McMichael C et al. (2008) Fire, climate change and biodiversity in Amazonia: A late-Holocene perspective. *Philisophical Transactions of the Royal Society B* 363: 1795–1802.

Carcaillet C (2001) Are Holocene wood-charcoal fragments stratified in alpine and subalpine soils? Evidence from the Alps based on AMS ^{14}C dates. *The Holocene* 11: 231–242.

Chepstow-Lusty AJ, Bennett KD, Fjeldsa J et al. (1998) Tracing 4,000 years of environmental history in the Cuzco area, Peru, from the pollen record. *Mountain Research and Development* 18: 159–172.

Cleveland WS and Devlin SJ (1988) Locally weighted regression: An approach to regression analysis by local fitting. *Journal of the American Statistical Association* 83: 596–610.

Cordiero RC, Turcq B, Suguio K et al. (2008) Holocene fires in East Amazonia (Carajás), new evidences, chronology and relation with paleoclimate. *Global and Planetary Change* 61: 49–62.

Denevan WM (ed.) (1992) *The Native Population of the Americas in 1492.* Second edition. University of Wisconsin Press.

Dull R, Nevle RJ, Woods WI et al. (2010) The Columbian encounter and the Little Ice Age: Abrupt land use change, rire, and greenhouse forcing. *Annals of the Association of American Geographers* 4: 755–771.

Erickson CL (2000) An artificial landscape-scale fishery in the Bolivian Amazon. *Nature* 408: 190–193.

Etheridge DM, Steele LP, Langenfelds RL et al. (2001) *Law Dome Atmospheric CO_2 Data*. IGBP PAGES/World Data Center for Paleoclimatology Data Contribution Series No. 2001-083, Boulder CO: NOAA/NGDC Paleoclimatology Program, Available online at ftp://ftp.ncdc.noaa.gov/pub/data/paleo/icecore/antarctica/law/law_co2.txt

Faust FX, Gnecco C, Mannstein H et al. (2006) Evidence for the postconquest demographic collapse of the Americas in historical CO_2 levels. *Earth Interactions* 10: 1–14.

Ferretti DF, Miller JB, White JWC et al. (2005) Unexpected changes to the global methane budget over the past 2000 years. *Science* 309: 1714–1717.

Food and Agriculture Organization (2007) *Fire Management: Global Assessment 2006*. FAO Forestry Paper 0258–6150. Food and Agriculture Organization of the United Nations, 151 pp.

Frank DC, Esper J, Raible CC et al. (2010) Ensemble reconstruction constraints on the global carbon cycle sensitivity to climate. *Nature* 463: 527–530.

Fuller JL (1997) Holocene forest dynamics in southern Ontaria, Canada: Fine-resolution pollen data. *Canadian Journal of Botany* 75: 1714–1727.

Garreaud RD, Vuille M, Compagnucci R et al. (2009) Present-day South American climate. *Palaeogeography, Palaeoclimatology, Palaeoecology* 281: 180–195.

Goldwijk KK, Beusen A and Janssen P (2010) Long-term dynamic modeling of global population and built-up area in a spatially explicit way: HYDE 3.1. *The Holocene* 20: 565–573.

Haberzettl T, Wille M, Fey M et al. (2006) Environmental change and fire history of southern Patagonia (Argentina) during the last five centuries. *Quaternary International* 158: 72–82.

Harrison SP, Marlon JR and Bartlein PJ (2010) Fire in the Earth System. In: Dodson J (ed.) *Changing Climates, Earth Systems and Society*. Springer, Chapter 3.

Haug GH, Hughen KA, Sigman DM et al. (2001) Southward migration of the Intertropical Convergence Zone through the Holocene. *Science* 293: 1304–1308.

Heckenberger MJ, Kuikuro A, Kuikuro UT et al. (2003) Amazonia 1492: Pristine forest or cultural parkland? *Science* 301: 1710–1714.

Jones PD and Mann ME (2004) Climate over past millennia. *Review of Geophysics* 42: RG2002, doi:10.1029/2003RG000143.

Joos F and Spahni R (2008) Rates of change in natural and anthropogenic radiative forcing over the past 20,000 years. *Proceedings of the National Academy of Sciences* 105: 1425–1430.

MacFarling Meuere C, Etheridge D, Trudinger C et al. (2006) Law Dome CO_2, CH_4 and N_2O ice core records extended to 2000 years BP. *Geophysical Research Letters* 33: L14810 doi:10.1029/2006GL026152.

Mann ME, Zhang Z, Rutherford S et al. (2009) Global signatures and dynamical origins of the Little Ice Age and Medieval Climate Anomaly. *Science* 326: 1256–1260.

Marlon JR, Bartlein PJ, Carcaillet C et al. (2008) A climate-driven decline in global biomass burning during the past two millennia. *Nature Geosciences* 1: 697–702.

Marlon JR, Bartlein PJ, Gavin DG et al. (2012) Long-term perspective on wildfires in the western USA. *Proceedings of the National Academy of Sciences of the United States of America* 109: 535–543.

Mayr C, Fey M, Haberzettl T et al. (2005) Palaeoenvironmental changes in southern Patagonia during the last millennium recorded in lake sediments from Laguna Azul (Argentina). *Palaeogeography, Palaeoclimatology, Palaeoecology* 228: 203–227.

Meyer I and Wagner S (2009) *The Little Ice Age in Southern South America: Proxy and Model Based Evidence*. In: Vimeux F, Sylvestre F and Khodri M (eds) *Past Climate Variability in South America and Surrounding Regions: From the Last Glacial Maximum to the Holocene*. Springer, pp. 395–412.

Mischler JA, Sowers TA, Alley RB et al. (2009) Carbon and hydrogen isotopic composition of methane over the last 1000 years. *Global Biogeochemical Cycles* 23: 1–13.

Monnin E, Steig EJ, Siegenthaler U et al. (2004) Evidence for substantial accumulation rate variability in Antarctica during the Holocene, through synchronization of CO_2 in the Taylor Dome, Dome C and DML ice cores. Earth and Planetary Science Letters *224: 45–54*.

Mooney SD, Harrison SP, Bartlein PJ et al. (2011) Late Quaternary fire regimes of Australasia. *Quaternary Science Reviews* 20: 28–46.

Moy CM, Dunbar RB, Moreno PI et al. (2008) Isotopic evidence for hydrologic change related to the westerlies in SW Patagonia, Chile, during the last millennium. *Quaternary Science Reviews* 27: 1335–1349.

Nepstad D, Lefebvre P, Da Silva UL et al. (2004) Amazon drought and its implications for forest flammability and tree growth: A basin-wide analysis. *Global Change Biology* 10: 704–717.

Nevle RJ and Bird DK (2008) Effects of syn-pandemic fire reduction and reforestation in the tropical Americas on atmospheric CO_2 during European conquest. *Palaeogeography, Palaeoclimatology, Palaeoecology* 264: 25–38.

NGRIP Dating Group 2006 (2005) *Greenland Ice Core Chronology (GICC05).* IGBP PAGES/World Data Center for Paleoclimatology Data Contribution Series # 2006-118. Boulder CO: NOAA/NCDC Paleoclimatology Program.

Niemann H and Behling H (2008) Late Quaternary vegetation, climate and fire dynamics inferred from the El Tiro record in the southeastern Ecuadorian Andes. *Journal of Quaternary Science* 23: 203–212.

Pechony O and Shindell DT (2010) Driving forces of global wildfires over the past millennium and the forthcoming century. *Proceedings of the National Academy of Sciences* 107: 19,167–19,170.

Pongratz J, Reick CH, Raddatz T et al. (2011) Past land use decisions have increased mitigation potential of reforestation. *Geophysical Research Letters* 38: 1–5.

Power MJ, Marlon JR, Bartlein PJ et al. (2010) Fire history and the global charcoal database: A new tool for hypothesis testing and data exploration. *Palaeogeography, Palaeoclimatology, Palaeoecology* 291(1–2): 52–59.

Power MJ, Marlon J, Ortiz N et al. (2008) Changes in fire regime since the Last Glacial Maximum: An assessment based on a global synthesis and analysis of charcoal data. *Climate Dynamics* 30: 887–907.

Ruddiman WF, Kutzbach JE and Vavrus SJ (2011) Can natural or anthropogenic explanations of late-Holocene CO_2 and CH_4 increases be falsified? *The Holocene* 21: 865–879.

Rue D, Webster D and Traverse A (2002) Late Holocene fire and agriculture in the Copan Valley, Honduras. *Ancient Mesoamerica* 13: 267–272.

Sceicz J, Zeeb BA, Bennett KD et al. (1998) High-resolution paleoecological analysis of recent disturbance in a southern Chilean *Nothofagus* forest. *Journal of Paleolimnology* 20: 235–252.

Siegenthaler U, Monnin E, Kawamura K et al. (2005) Supporting evidence from the EPICA Dronning Maud Land ice core for atmospheric CO_2 changes during the past millennium. *Tellus B* 57: 51–57.

Simard I, Morin H and Lavoie C (2006) A millennial-scale reconstruction of spruce budworm abundance in Saguenay, Quebec, Canada. *The Holocene* 16: 31–37.

Stocker BD, Strassmann K and Joos F (2011) Sensitivity of Holocene atmospheric CO_2 and the modern carbon budget to early human land use: Analyses with a process-based model. *Biogeosciences* 8: 69–88.

Stuiver M, Braziunas TF, Grootes PM et al. (1997) Is there evidence for solar forcing of climate in the GISP2 oxygen isotope record? *Quaternary Research* 48: 259–266.

Thompson LG, Mosley-Thompson E, Bolzan JF et al. (1985) A 1500 year record of climate variability recorded in ice cores from the tropical Quelccaya Ice Cap. *Science* 229: 971–973.

Vannière B, Power MJ, Roberts N et al. (2011) Circum-Mediterranean fire activity and climate changes during the mid-Holocene environmental transition (8500–2500 cal. BP). *The Holocene* 21: 53–73.

Wang Z, Chappellaz J, Park K et al. (2010) Large variations in Southern Hemisphere biomass burning during the last 650 years. *Science* 330: 1663–1666.